First-principles investigation of alternating current density distribution in molecular devices

Lei Zhang,[1] Bin Wang,[2,1] and Jian Wang[1,*]

[1]*Department of Physics and the Center of Theoretical and Computational Physics, The University of Hong Kong, Pokfulam Road, Hong Kong, China*

[2]*Department of Physics and Institute of Computational Condense Matter Physics, Shenzhen University, Shenzhen 518060, China*

(Received 20 May 2012; revised manuscript received 4 October 2012; published 19 October 2012)

Using the nonequilibrium Green's function (NEGF) formalism, we derive the current density formula for ac quantum transport by including the self-consistent Coulomb interaction. It is well known that the Coulomb interaction is very important in determining ac current in nanostructures. As pointed out by Büttiker that the Coulomb interaction must be included to conserve the ac current. Theoretically, the displacement current can be accounted for by including a self-consistent Hartree term in the Hamiltonian as well as the exchange and correlation term while the ac current is calculated from particle current, i.e., $\langle \hat{I}_\alpha(t)\rangle = q\langle d\hat{N}_\alpha/dt\rangle$ where $\hat{N}_\alpha$ is the number operator of the α lead. For the ac current density, however, the Coulomb interaction contributes in two ways. As the case of ac current, the self-consistent Coulomb interaction has to be included in the conventional particle current density. In addition, we have to consider the displacement current density explicitly, which is proportional to the time derivative of displacement field. Once the ac current density is obtained, one can calculate the ac current by integrating it over a cross-section area along the transport direction. It is shown that ac current obtained from the total ac current density is conserved and equal to that calculated directly from the lead using NEGF theory. We have applied our formalism to calculate ac current density for nanodevices by combining the density functional theory (DFT) with NEGF theory. Specifically, we have calculated the ac current density to the first order of frequency in a molecular device Al-C_4-Al from first principles. It is found that Al-C_4-Al system exhibits inductive-like behavior under ac bias in the low-frequency limit. Furthermore, nonequilibrium charge distribution is obtained that enables us to study electrochemical capacitance of the molecular devices.

DOI: 10.1103/PhysRevB.86.165431 PACS number(s): 72.10.Bg, 73.63.−b, 85.65.+h

I. INTRODUCTION

Anticipating the future high-speed electronic devices, huge research efforts have been made on understanding physical processes of time-dependent quantum transport in coherent mesoscopic systems or nanostructures.[1–20] On the experimental side, there exist many interesting phenomena in ac quantum transport such as charge relaxation resistance. Charge relaxation resistance is predicted to be the half of the resistance quanta in theory[1] and is experimentally realized on a 2D electron gas.[10] Recently, an on-demand single-electron source was realized experimentally so that a single electron is emitted and reabsorbed periodically on the time scale of nanoseconds thereby generating quantized alternating current.[11] Most recently, a single-electron detector to capture this single-electron source has been demonstrated by two experimental groups making on-demand single-electron source a promising candidate for 2DEG quantum computer.[12,13] As to the possible device applications, the performance of nanotube transistors under high frequency was studied in Refs. 17–19 and the results indicate that there is little decrease in performance up to gigahertz (GHz) frequencies for the nanotube.

On the theoretical side, because the quantum transport problem under the time varying ac bias is complicated owing to the presence of displacement current in the system, several methods have been developed to tackle this problem, such as scattering matrix theory,[2–4] and NEGF formalism.[5,6,20–23] It was recognized that the displacement current must be added to conserve the current.[2–4] For ac transport, the total ac current consists of two contributions: the conduction current defined as rate of change of charge flow and the displacement current, which is the rate of change of displacement field. Theoretically, the conduction current can be easily calculated from the lead while the displacement current can be defined in the scattering region. Although all the terminal ac currents calculated so far used the definition of the conductance current, the displacement current has been included implicitly in the following way. Since the displacement current is due to the Coulomb interaction, it turns out that by including a self-consistent Coulomb interaction term into the Hamiltonian the conduction ac current is conserved.[3,23] In another word, there is no need to include displacement current explicitly in the current operator. Note that this is valid only for the global ac quantities such as dynamic conductance or ac current. For ac current density, however, the displacement current density must be included explicitly as we will show in this paper. While most of the previous studies focus on the dynamic conductance, it is also very interesting to investigate the ac current density profile. Such a study is important to gain further insight into the dynamic transport processes of quantum systems. Specifically the current density distribution can present a vivid picture of how the current flows inside the central region, it can also provide detailed local transport information as well. Finally, the current density profile can provide important information on local heating when a dissipative mechanism exists in the quantum system.

In this paper, we have developed a theoretical formalism to calculate the ac current density using a nonequilibrium Green's function method. We are interested in the regime where the Coulomb blockade effect is not important.[24] By explicitly including displacement current density and Coulomb interaction, we show that the ac current density is a conserved quantity. We further prove that the current obtained by integrating the ac current density over a cross-section area along the

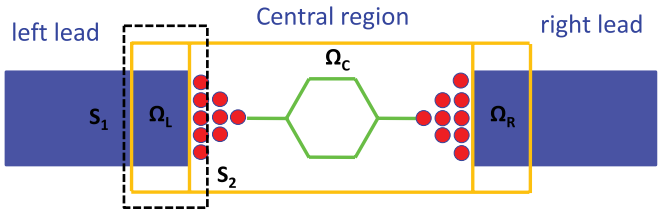

FIG. 1. (Color online) A sketch illustrating the two-terminal device. Central region is our simulation box and it contains $\Omega_{L/R}$ and Ω_C regions. The $\Omega_{L/R}$ is self-energy coupling region due to the external leads. The Ω_C region represents the molecular device. $\mathbf{S}_1/\mathbf{S}_2$ is an arbitrary surface outside of the left lead and inside Ω_C region.

transport direction is equal to the ac terminal current. Finally, we note that most of the theoretical ac transport investigations concentrate on the mesoscopic system, less attention has been paid on atomic systems.[29,30] In this paper, we have combined the nonequilibrium Green's function method with the density functional theory allowing us to calculate the ac *current density* in the small bias voltage and frequency for an atomic junction from first principles.

The paper is organized as follows. In Sec. II, basic formulas for calculating ac current density are derived by using the nonequilibrium Green's function method (NEGF) and taking into account the self-consistent Coulomb interaction in the system. As an example, the ac current density to the first order in frequency (Ω) is numerically calculated in Sec. III. We have also given techniques details and numerical analysis of results for a molecular device Al-C_4-Al. In Sec. IV, summary is given.

II. THEORETICAL FORMALISM

We start from a typical two-terminal device shown in Fig. 1, which consists of the central scattering region coupled with two external leads where ac bias $v_\alpha(t) = v_\alpha \cos(\omega t)$ is applied. Under the ac bias, the conventional current density is defined as

$$\mathbf{J}_c(\mathbf{r},t) = -\frac{i\hbar}{2m}[(\nabla - \nabla')\rho(\mathbf{r},\mathbf{r}',t)]_{\mathbf{r}'=\mathbf{r}}. \tag{1}$$

Taking the Fourier transform of Eq. (1), we have $\mathbf{J}_c(\mathbf{r},\Omega) = -\frac{i\hbar}{2m}[(\nabla - \nabla')\rho(\mathbf{r},\mathbf{r}',\Omega)]_{\mathbf{r}'=\mathbf{r}}$, where Ω is the response frequency. Because the charge density matrix can be expressed in terms of lesser Green's function $\rho(\Omega) = iq\int dE/(2\pi)G^<(E_+,E)$ with $E_+ = E + \hbar\Omega$, the conventional current density $\mathbf{J}_c(\mathbf{r},\Omega)$ can be expressed using lesser Green's function:

$$\mathbf{J}_c(\mathbf{r},\Omega) = \frac{q\hbar}{2m}\int \frac{dE}{2\pi}[(\nabla - \nabla')G^<(\mathbf{r},\mathbf{r}',E_+,E)]_{\mathbf{r}'=\mathbf{r}}. \tag{2}$$

Note that in the presence of ac bias, the translational symmetry in time is broken and the Green's function depends on double time indices.

In this work, we are interested in the limit of small ac bias voltage. In this case, the nonequilibrium lesser Green's function $G^<$ can be expanded to the first order in v_α:[21–23]

$$G^< = G_0^< + g^<, \tag{3}$$

where $G_0^<$ is the equilibrium Green's function and $g^<$ is the first-order nonequilibrium correction due to the ac bias. Because the current calculated from the equilibrium $G_0^<$ is zero, only ac current density generated by the first-order term $g^<$ will be considered below. Then, we have

$$\mathbf{J}_c(\mathbf{r},\Omega) = \frac{q\hbar}{2m}\int \frac{dE}{2\pi}[(\nabla - \nabla')g^<(\mathbf{r},\mathbf{r}',E_+,E)]_{\mathbf{r}'=\mathbf{r}}. \tag{4}$$

In the wide-band limit, the first-order correction of lesser Green's function is given by[23]

$$g^<(E_+,E) = iq\sum_\alpha \frac{f-\bar{f}}{\Omega}\bar{G}^r\Gamma_\alpha G^a v_\alpha(\Omega) + iq\bar{G}^r U_1 G^r \Gamma G^a f + iq\bar{G}^r\Gamma\bar{G}^a U_1 G^a \bar{f}, \tag{5}$$

where the subscript $\alpha = L,R$ denotes the corresponding left or right lead respectively; $v_\alpha(\Omega) = \pi v_\alpha[\delta(\Omega+\omega) + \delta(\Omega-\omega)]$; and $\Gamma_\alpha = i(\Sigma_\alpha^r - \Sigma_\alpha^a)$ is the linewidth function. For simplicity, the abbreviations $\bar{G}^r \equiv G^r(E_+)$ and $\bar{f} \equiv f(E_+)$ are used with $E_+ = E + \hbar\Omega$; $U_1(\Omega) = \sum_\alpha u_\alpha(\Omega)v_\alpha(\Omega)$ is the first-order Coulomb interaction due to the ac external bias. Here, $u_\alpha(\Omega)$ is the frequency-dependent characteristic potential, which describes the first-order internal response due to the ac bias and is determined by the Poisson-like equation:

$$\nabla^2 u_\alpha(\mathbf{r},\Omega) = -4\pi\rho_\alpha(\mathbf{r},\Omega) = -4\pi q^2\frac{dn_\alpha(\mathbf{r},\Omega)}{dE} + 4\pi q^2\frac{dn(\mathbf{r},\Omega)}{dE}u_\alpha(\mathbf{r},\Omega), \tag{6}$$

where we have used the Thomas-Fermi approximation. Here, the frequency-dependent injectivity $dn_\alpha(\mathbf{r},\Omega)/dE$ is defined as[14,15]

$$\frac{dn_\alpha(\mathbf{r},\Omega)}{dE} = \int \frac{dE}{2\pi}\frac{f-\bar{f}}{\Omega}[\bar{G}^r\Gamma_\alpha G^a]_{\mathbf{rr}}, \tag{7}$$

with $dn(\mathbf{r},\Omega)/dE = \sum_\alpha dn_\alpha(\mathbf{r},\Omega)/dE$. The equilibrium retarded Green's function is defined as

$$G^r(E) = \frac{1}{E - H_0 - qU_{\rm eq} - \Sigma_0^r(E)}, \tag{8}$$

where H_0 contains all parts of the Hamiltonian including exchange and correlation energy except the equilibrium Hartree potential $U_{\rm eq}$ and $\Sigma_0^r(E)$ is the equilibrium self-energy due to the external leads. It is straightforward to show that

$$\rho(\mathbf{r},\Omega) = \sum_\alpha \rho_\alpha(\mathbf{r},\Omega)v_\alpha(\Omega) = iq\int (dE/2\pi)[g^<(E_+,E,\mathbf{r},\mathbf{r}')]_{\mathbf{r}'=\mathbf{r}}, \tag{9}$$

is the nonequilibrium charge distribution up to first order in ac bias. In real materials, electrodes are metallic conductors, which will screen off the electric field over distances of the Thomas-Fermi screening length. This allows us to choose a large enough central scattering region $\Omega_{L/R} + \Omega_C$ (see Fig. 1) such that there will be no electric field lines penetrating the surface of the central scattering region. According to Gauss theorem, the total charge in the central scattering region is zero, which is exactly the boundary condition in solving Eq. (6). In the *ab initio* calculation, we found that when the length of buffer layer is three or four unit cells, the electric field will be screened off. In the ac transport theory, we have implicitly made an approximation that the potential of the

electrode shifts according to the ac bias. This is the so-called adiabatic approximation (see Ref. 6) so that the frequency of the bias cannot be too high. In Ref. 6, the estimated upper limit frequency is quite high, around tetrahertz.

With the characteristic potential and lesser Green's function obtained, we can calculate the conventional ac current density using Eq. (4). This, in turn, allows us to calculate the ac current by integrating current density over arbitrary cross-section inside the scattering region perpendicular to the transport direction, e.g., $\mathbf{S}_2$ in Fig. 1. It is known that in the presence of ac bias, the following continuity equation must be satisfied:

$$\nabla \cdot \mathbf{J}_c(\mathbf{r},t) + \partial\rho(\mathbf{r},t)/\partial t = 0. \tag{10}$$

If we integrate this equation over a large volume enclosing the central scattering region, we have

$$I_L(t) + I_R(t) = 0, \tag{11}$$

where we have used the fact that once the Poisson-like equation Eq. (6) is solved, we have $\int \rho(\mathbf{r},t)d\mathbf{r} = 0$ due to the boundary condition and $I_L = \int d\mathbf{S}_1 \cdot \mathbf{J}_c(\mathbf{r},t)$. Hence, once the Coulomb interaction is included, the conventional current density will give the conserved ac current. However, if we are interested in the local quantity, i.e., ac current density, care must be taken since the second term in Eq. (10) also contributes to the ac current density. Furthermore, if we wish to implement our theoretical formalism in the first-principles calculation, we may have to worry about nonlocal potentials.[31] Because the nonlocal potential appears in the first-principles calculation such as the nonlocal pseudopotential, one has to introduce another current density $\mathbf{J}_{\rm nl}(\mathbf{r})$ to get a conserved current density. Similar to the static nonlocal current density discussed in Refs. 31 and 32, we introduce a nonequilibrium nonlocal current density $\mathbf{J}_{\rm nl}(\mathbf{r})$:

$$\mathbf{J}_{\rm nl}(\mathbf{r},\Omega) = -\nabla\phi(\mathbf{r},\Omega), \tag{12}$$

with

$$-\nabla^2\phi(\mathbf{r},\Omega) = \rho_n(\mathbf{r},\Omega), \tag{13}$$

where $\rho_n(\mathbf{r},\Omega)$ is the nonlocal electron density and is defined as

$$\rho_n(\mathbf{r},\Omega) = -\frac{q}{h}\int d\mathbf{r}'[V_{\rm nl}(\mathbf{r},\mathbf{r}')g^<(E_+,E) - \text{c.c.}], \tag{14}$$

where $V_{\rm nl}(\mathbf{r},\mathbf{r}')$ is the nonlocal potential in the Hamiltonian. Obviously, $\rho_n(\mathbf{r},\Omega) = 0$ if all the potentials are local.

Therefore, in the presence of nonlocal potential, the Fourier transformation of continuity equation should be modified as

$$\nabla \cdot \mathbf{J}_c(\mathbf{r},\Omega) + \rho_n(\mathbf{r},\Omega) - i\Omega\rho(\mathbf{r},\Omega) = 0. \tag{15}$$

From Eqs. (6) and (9), we have $\nabla^2 U_1(\mathbf{r},\Omega) = -4\pi\rho(\mathbf{r},\Omega)$. Hence we identify the displacement current density corresponding to the third term in Eq. (15) as $\mathbf{J}_d(\Omega) = i\frac{\Omega}{4\pi}\nabla U_1(\Omega)$. Note that this expression is consistent with the classical physics, where the displacement current density is defined as

$$\mathbf{J}_d(\Omega) = -\frac{i}{4\pi}\Omega\mathbf{D}, \tag{16}$$

and the displacement field $\mathbf{D}$ is $\mathbf{D} = -\nabla U_1(\Omega)$. Hence the continuity equation (15) becomes

$$\nabla \cdot [\mathbf{J}_c(\mathbf{r},\Omega) + \mathbf{J}_{\rm nl}(\mathbf{r},\Omega) + \mathbf{J}_d(\mathbf{r},\Omega)] = \nabla \cdot \mathbf{J}_t(\mathbf{r},\Omega) = 0, \tag{17}$$

where we introduce the total current density $\mathbf{J}_t = \mathbf{J}_c + \mathbf{J}_{\rm nl} + \mathbf{J}_d$. We see that the total ac current density consists of conventional ac current density (which depends on Coulomb interaction), displacement current density and nonlocal current density if the Hamiltonian has nonlocal potential.

In the following, we will verify that the continuity equation Eq. (17) is indeed correct for the two-terminal device structure. Firstly, the divergence of conventional current density can be calculated as

$$\nabla \cdot \mathbf{J}_c(\mathbf{r},\Omega) = \frac{q\hbar}{2m}\int \frac{dE}{2\pi}[(\nabla^2 - \nabla'^2)g^<(\mathbf{r},\mathbf{r}',E,E_+)]_{\mathbf{r}'=\mathbf{r}}. \tag{18}$$

Combining Eq. (14) with Eq. (18), we have

$$\begin{aligned}\nabla \cdot [\mathbf{J}_c(\mathbf{r},\Omega) + \mathbf{J}_{\rm nl}(\mathbf{r},\Omega)] &= -\frac{q}{\hbar}\int \frac{dE}{2\pi}[Hg^< - g^<H]_{\mathbf{rr}} \\ &= -\frac{q}{\hbar}\int \frac{dE}{2\pi}[(H - E - \hbar\Omega)g^< - g^<(H - E - \hbar\Omega)]_{\mathbf{rr}},\end{aligned} \tag{19}$$

where $H = -\frac{\hbar^2}{2m}\nabla^2 + V(\mathbf{r}) + V_{\rm nl}(\mathbf{r},\mathbf{r}')$.

Using the relation $(I + \Sigma^r\bar{G}^r) = (E + \hbar\Omega - H)\bar{G}^r$ and its complex conjugate as well as Eq. (5), Eq. (19) becomes

$$\nabla \cdot [\mathbf{J}_c(\mathbf{r},\Omega) + \mathbf{J}_{\rm nl}(\mathbf{r},\Omega)] = \frac{iq^2}{\hbar}\sum_{i=1}^{5}[A_i]_{\mathbf{rr}} + B_{\mathbf{rr}}, \tag{20}$$

where we have defined several auxiliary matrices:

$$\begin{aligned}
A_{1\mathbf{rr}} &= \int \frac{dE}{2\pi}\sum_\alpha v_\alpha(\Omega)\frac{f-\bar{f}}{\Omega}[\Gamma_\alpha G^a - \bar{G}^r\Gamma_\alpha + \Sigma^r\bar{G}^r\Gamma_\alpha G^a - \bar{G}^r\Gamma_\alpha G^a\Sigma^a]_{\mathbf{rr}}, \\
A_{2\mathbf{rr}} &= \int \frac{dE}{2\pi}[\Sigma^r\bar{G}^r U_1 G^r\Gamma G^a f - \bar{G}^r U_1 G^r\Gamma G^a\Sigma^a f]_{\mathbf{rr}}, \quad A_{3\mathbf{rr}} = \int \frac{dE}{2\pi}[\Gamma\bar{G}^a U_1 G^a\bar{f} - \bar{G}^r U_1 G^r\Gamma f]_{\mathbf{rr}}, \\
A_{4\mathbf{rr}} &= \int \frac{dE}{2\pi}[\Sigma^r\bar{G}^r\Gamma\bar{G}^a U_1 G^a\bar{f} - \bar{G}^r\Gamma\bar{G}^a U_1 G^a\Sigma^a\bar{f}]_{\mathbf{rr}}, \quad A_{5\mathbf{rr}} = \int \frac{dE}{2\pi}[U_1 G^r\Gamma G^a f - \bar{G}^r\Gamma\bar{G}^a U_1\bar{f}]_{\mathbf{rr}}, \\
B_{\mathbf{rr}} &= -q\Omega\int \frac{dE}{2\pi}g^<(\mathbf{r},\mathbf{r},E_+,E) = i\Omega q^2\sum_\alpha\left[\frac{dn_\alpha(\mathbf{r},\Omega)}{dE} - \frac{dn(\mathbf{r},\Omega)}{dE}u_\alpha(\mathbf{r},\Omega)\right]v_\alpha(\Omega).
\end{aligned} \tag{21}$$

In the wide-band limit where the linewidth function does depend on energy, we have $A_{5\mathbf{rr}} = 0$. Therefore we have

$$\nabla \cdot \mathbf{J}_t(\mathbf{r},\Omega) = \nabla \cdot (\mathbf{J}_c + \mathbf{J}_{\rm nl} + \mathbf{J}_d) = i\Omega \sum_\alpha \left[\frac{1}{4\pi}\nabla^2 u_\alpha(\mathbf{r},\Omega) + q^2 \frac{dn_\alpha(\mathbf{r},\Omega)}{dE} - q^2 \frac{dn(\mathbf{r},\Omega)}{dE} u_\alpha(\mathbf{r},\Omega) \right] v_\alpha(\Omega) + \frac{iq^2}{\hbar} \sum_{i=1}^{4} [A_i]_{\mathbf{rr}}$$
$$= \frac{iq^2}{\hbar} \sum_{i=1}^{4} [A_i]_{\mathbf{rr}}, \tag{22}$$

where we have used Eq. (6) for the characteristic potential u_α. In the following, we will show that all A_i are zero in the region Ω_C depicted in Fig. 1.

As shown in Fig. 1, there are two different types of region in the central scattering region: the region Ω_C and the left and right lead coupling $\Omega_{L/R}$ region beyond which the self-energy is zero. In the NEGF-DFT simulations, the simulation box is $\Omega_t = \Omega_L + \Omega_R + \Omega_C$. However, when calculating the ac current density, we will restrict ourselves to the region Ω_C since only in this region the ac current density is conserved. This is due to the following reason. Because electrons come into or out of the central device region through the self-energy coupling region $\Omega_{L/R}$, which plays the role of the source and drain, $\nabla \cdot \mathbf{J}_t(\mathbf{r},\Omega)|_{\mathbf{r}\in\Omega_{L/R}} \neq 0$. Since the self-energy Σ^r_α is zero outside the coupling region $\Omega_{L/R}$, the terms A_i with $i = 1,\ldots,4$ all involve surface terms Γ or Σ^r and must be zero in Ω_C region. We therefore conclude that the total current density $\mathbf{J}_t$ is conserved in the central device region Ω_C, i.e., $\nabla \cdot \mathbf{J}_t(\mathbf{r},\Omega)|_{\mathbf{r}\in\Omega_C} = 0$.

Before carrying out numerical calculations, we wish to show that the current calculated from current density $\mathbf{J}_t$ is equal to the current calculated from Landauer-Buttiker type of dynamic conductance formula. Considering an arbitrary surface $\mathbf{S}_2$ inside of the central molecular device region Ω_C as shown in Fig. 1, we know that the current coming from the left lead can be calculated through

$$I_L(\Omega) = \int_{\mathbf{S}_2} \mathbf{J}_t(\mathbf{r},\Omega) \cdot d\mathbf{S}. \tag{23}$$

It is important to note that current density is only defined inside the central region in the NEGF formalism, which implies that the integration of $\mathbf{J}_t$ over the surface $\mathbf{S}_1$ outside of central region is zero. Therefore we can consider a closed surface $\mathbf{S}$ that encloses part of the scattering region (Ω_L) with $\mathbf{S}_1$ and $\mathbf{S}_2$ just outside of the left lead coupling region. Since surface $\mathbf{S}_1$ does not contribute to the current, the current expression becomes

$$I_L(\Omega) = \int_{\mathbf{S}} \mathbf{J}_t(\mathbf{r},\Omega) \cdot d\mathbf{S} = \int_{\Omega_L} \nabla \cdot \mathbf{J}_t(\mathbf{r},\Omega). \tag{24}$$

Note that $\nabla \cdot \mathbf{J}_t(\mathbf{r},\Omega)$ is given by Eq. (22), which is nonzero in the coupling region Ω_L. Let us consider a typical term in Eq. (22), e.g., the first term in expression A_2. Using the fact that Σ^r equals to Σ^r_L in Ω_L, we have $\Sigma^r \bar{G}^r U_1 G^r \Gamma G^a f = \Sigma^r_L \bar{G}^r U_1 G^r \Gamma G^a f \equiv A_0$. Since Σ^r_L is zero outside of Ω_L, the trace of Ω_L in Eq. (24) can be expanded to the whole scattering region Ω_t, i.e., $\mathrm{Tr}[A_0]_{\Omega_L} = \mathrm{Tr}[A_0]_{\Omega_t}$. The other terms in A_i can be treated similarly. After some algebra, we have

$$I_L(\Omega) = \mathrm{Tr}[\nabla \cdot \mathbf{J}_t(\mathbf{r},\Omega)]_{\Omega_L} = \mathrm{Tr}[\nabla \cdot \mathbf{J}_t(\mathbf{r},\Omega)]_{\Omega_t}$$
$$= -\frac{q^2}{\hbar} \int \frac{dE}{2\pi} \frac{f-\bar{f}}{\Omega} \mathrm{Tr}[i(\bar{G}^r - G^a)\Gamma_L v_L(\Omega)$$
$$- \bar{G}^r \sum_\beta \Gamma_\beta v_\beta(\Omega) G^a \Gamma_L + i\Omega \Gamma_L \bar{G}^r U_1(\Omega) G^a], \tag{25}$$

which agrees with the dynamic conductance calculated from the lead using the standard NEGF method.[23]

This shows that as long as the surface $\mathbf{S}_2$ is not inside the self-energy coupling regions Ω_L and Ω_R, the integration of current density over $\mathbf{S}_2$ is equal to the current calculated from the lead. Note that due to the different definitions of current operator, there is a sign difference between our approach and that of scattering matrix theory of Buttiker. In Sec. III, we will use the definition of Buttiker to discuss the physics of numerical results.

Finally, we note that the Coulomb interaction plays an important role in ac transport and is responsible for the displacement current. For ac current density, the displacement current appears in two places: (1) the Coulomb interaction term U_1 in Eq. (5); (2) the displacement current density $\mathbf{J}_d$ in Eq. (16). This is different from ac terminal current where the displacement current is not explicitly considered. All we have to do for ac current is to calculate the particle current from the leads while considering the Coulomb interaction explicitly. Here, both terms have to be included in order to conserve the ac current *density*.

III. NUMERICAL CALCULATION OF AC CURRENT DENSITY

Now, we discuss how to numerically calculate ac current density from first principles. To begin with, we rewrite Eq. (5) as

$$g^<(E_+,E) = iq\frac{f-\bar{f}}{\Omega} \sum_\alpha [\bar{G}^r \Gamma_\alpha G^a - \bar{G}^r \Gamma G^a u_\alpha] v_\alpha(\Omega)$$
$$= iq\frac{f-\bar{f}}{\Omega} \{\bar{G}^r \Gamma G^a [1 - u_L - u_R] v_R(\Omega)$$
$$+ [\bar{G}^r \Gamma_L G^a - \bar{G}^r \Gamma G^a u_L][v_L(\Omega) - v_R(\Omega)]\}. \tag{26}$$

Since $\sum_\alpha u_\alpha = 1$, only the second term is the nonequilibrium part.

In the molecular electronics, the energy scale is electron volt, which corresponds to 1000 THz. Therefore the second order in the expansion of $\hbar\omega/E$ can be safely neglected for

gigahertz-frequency range. As an application of our formalism, we wish to calculate ac current density in the low-frequency limit as an illustration. Therefore we expand Eq. (5) to the first order in frequency Ω and only consider a dynamical term by getting rid of dc terms ($\Omega = 0$). In the following, the differential current density will be considered, which is defined as current density divided by the voltage difference $\delta v(\Omega) = v_L(\Omega) - v_R(\Omega)$. Then, the differential conventional current density coming from the left lead can be written as (see Appendix)

$$\begin{aligned}&\mathbf{J}_c(\mathbf{r},\Omega)\\&= \frac{iq^2\hbar\Omega}{4m}\int\frac{dE}{2\pi}(-\partial_E f)[(\nabla-\nabla')(G^r\Gamma_L G^a G^a\\&\quad - G^r G^r\Gamma_L G^a + (G^r G^r\Gamma G^a - G^r\Gamma G^a G^a)_{\mathbf{rr}}u_L)]_{\mathbf{r}'=\mathbf{r}},\end{aligned} \tag{27}$$

where the characteristic potential u_L is frequency independent if we only consider the first-order effect. Furthermore, the Thomas-Fermi approximation[3,23] is adopted, which assumes that only the local response is considered, the frequency independent characteristic potential (6) becomes

$$\nabla^2 u_\alpha(\mathbf{r}) = -4\pi q^2\frac{dn_\alpha(\mathbf{r})}{dE} + 4\pi q^2\frac{dn(\mathbf{r})}{dE}u_\alpha(\mathbf{r}), \tag{28}$$

where frequency independent injectivity is defined as

$$\frac{dn_\alpha(\mathbf{r})}{dE} = \int\frac{dE}{2\pi}(-\partial_E f)[G^r\Gamma_\alpha G^a]_{\mathbf{rr}} \tag{29}$$

and the local density of states $dn/dE = \sum_\alpha dn_\alpha/dE$. For the boundary condition of Poisson-like equation (28), because the total charge in the whole scattering region is zero, we have $\int\nabla\cdot\mathbf{J}_d(\mathbf{r})d\mathbf{r} = \int\mathbf{J}_d(\mathbf{r})\cdot d\mathbf{S} = 0$. Hence a reasonable boundary condition should be $\hat{\mathbf{n}}\cdot\mathbf{J}_d(\mathbf{r}) = 0$ or, equivalently, $\hat{\mathbf{n}}\cdot\partial u_\alpha(\mathbf{r}) = 0$, where $\hat{\mathbf{n}}$ is the normal direction of the interface at the boundary.

At zero temperature, the conventional current density becomes

$$\begin{aligned}&\mathbf{J}_c(\mathbf{r},\Omega)\\&= \frac{iq^2\hbar\Omega}{8\pi m}(\nabla-\nabla')[G^r\Gamma_L G^a G^a - G^r G^r\Gamma_L G^a\\&\quad + (G^r G^r\Gamma G^a)_{\mathbf{rr}}u_L(\mathbf{r}) - (G^r\Gamma G^a G^a)_{\mathbf{rr}}u_L(\mathbf{r})]_{\mathbf{r}'=\mathbf{r}},\end{aligned} \tag{30}$$

where $G^r(E)$ is evaluated using Eq. (8) with $E = E_f$. Correspondingly, the first order of differential displacement current density is defined as

$$\mathbf{J}_d(\mathbf{r},\Omega) = \frac{i\Omega}{4\pi}\nabla u_L. \tag{31}$$

The nonlocal current density $\mathbf{J}_{\rm nl}$ can be calculated using Eqs. (12) and (13) with the nonlocal electron density $\rho_n(\mathbf{r})$:[32]

$$\rho_n(\mathbf{r}) = \nabla\cdot\mathbf{J}_t(\mathbf{r}) - \nabla\cdot\mathbf{J}_c(\mathbf{r}) - \nabla\cdot\mathbf{J}_d(\mathbf{r}), \tag{32}$$

where $\nabla\cdot\mathbf{J}_t(\mathbf{r})$ is given by

$$\begin{aligned}&\nabla\cdot\mathbf{J}_t(\mathbf{r},\Omega)\\&= -\frac{iq^2\Omega}{h}\mathrm{Re}[\Sigma^r G^r G^r\Gamma_L G^a - (1+\Sigma^r G^r)\Gamma_L G^a G^a\\&\quad + ((1+\Sigma^r G^r)\Gamma G^a G^a - \Sigma^r G^r G^r\Gamma G^a)_{\mathbf{rr}}u_L(\mathbf{r})]_{\mathbf{rr}}.\end{aligned} \tag{33}$$

Furthermore, it is easy to check that

$$\mathrm{Tr}[\nabla\cdot\mathbf{J}_t(\mathbf{r},\Omega)]_{\Omega_L} = i\Omega E_{LL} = \frac{iq^2\Omega}{h}\mathrm{Tr}\left[\frac{dn_{LL}}{dE} - \frac{dn_L}{dE}u_L\right], \tag{34}$$

where $E_{\alpha\beta}$ is emittance that describes the low-frequency response of the system and LPDOS dn_{LL}/dE is defined as[3]

$$\frac{dn_{LL}(\mathbf{r})}{dE} = \mathrm{Re}[(G^r\Gamma_L G^r + iG^r\Gamma_L G^a\Gamma_L G^r)_{\mathbf{rr}}]. \tag{35}$$

To summarize the calculation procedure, the characteristic potential (28) for u_L should be solved firstly. Secondly, we calculate the conventional current density $\mathbf{J}_c$ and the displacement current density $\mathbf{J}_d$ using Eqs. (30) and (31), respectively, and their divergence. The divergence of the total current density can also be calculated from Eq. (33). Thirdly, we then calculate the nonlocal electron density using Eq. (32) and the nonlocal current density can be obtained from Eqs. (12) and (13). Finally, the total current density $\mathbf{J}_t$ can be obtained by summing up all three components.

In the following, we will present our numerical results of the ac current density of the molecular Al-C_4-Al device. Our numerical analysis uses the state-of-the-art first-principles quantum transport package MATDCAL.[33–35] In particular, a linear combination of atomic orbitals (LCAO) is employed to KS equations. The exchange-correlation is treated at the LDA level and the nonlocal norm-conserving pseudopotential[36] is used to define the atomic core. The density matrix is constructed in orbital space and the effective potential is obtained in real space by solving the Poisson equation. The accuracy in the self-consistent iteration is numerically converged to 10^{-4} eV. Figure 2 depicts the atomic structure Al-C_4-Al system. There are 18 atoms in a unit cell with a finite cross section along (100) direction in the semi-infinite Al electrodes. The distance between the carbon atoms is fixed to 2.5 a.u. and that between the carbon wire and the Al electrode is 3.78 a.u. There are 76 atoms in the cental scattering region.

Once the NEGF-DFT self-consistency is reached as the numerical tolerance is less than 10^{-4} eV, we obtain the self-consistent Hamiltonian and Green's function defined in orbital space. Notice that the current density is defined in real space, the transformation from the orbital space to the real space should be done as in Ref. 32.

In order to calculate the ac current density, the characteristic potential (28) should be solved. The characteristic potential u_L and u_R across the cross section located at z are defined

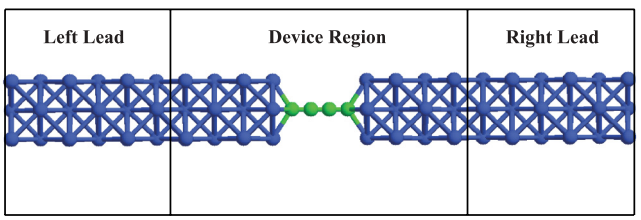

FIG. 2. (Color online) Schematic diagram of a molecular device Al-C_4-Al. The device consists of a four-carbon-atoms chain coupled to the perfect aluminium atomic electrodes, which will extend to the reservoirs at $\pm\infty$, where the current is collected.

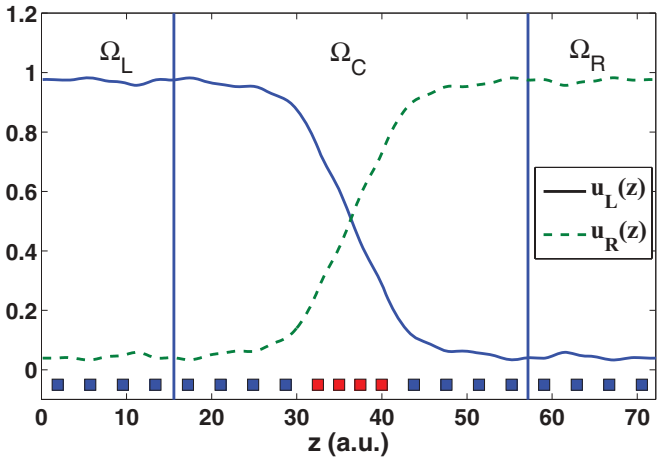

FIG. 3. (Color online) The characteristic potential distribution $u_L(z)$ (blue solid line) and $u_R(z)$ (green dashed line) along the transport z direction. Blue square points represent Al atoms and red square points represent C atoms.

as $u_\alpha(z) = \int dxdy u_\alpha(\mathbf{r}), \alpha = L, R$ and are shown in Fig. 3. According to its definition, the characteristic potential reflects the response of the electrostatic potential inside the scattering region to the variation of the electrochemical potential μ_α inside electrode α.[23,37] We note that the Coulomb potential consists of two parts: equilibrium (when bias is zero) and nonequilibrium parts. When the bias is nonzero, this nonequilibrium Coulomb potential is due to the interaction of injected charged with the system. In the linear bias regime, this potential is proportional to the bias with the coefficient called characteristic potential coined by Büttiker. To appreciate the physical meaning of the characteristic potential u_α, we vary the left electrochemical potential by setting v_R to zero and consider $u_L(Z)$ shown in Fig. 3. As we can see from Fig. 3, the characteristic potential $u_L(Z)$ deep inside Ω_L is almost constant and around 1, which indicates that the electrostatic potential deep inside Ω_L changes synchronously with the electrochemical potential change v_L in the left electrode. In addition, the screening effect is clearly seen. In the central scattering region, the electrostatic potential changes due to the variation of the left electrochemical potential, drops drastically from left to right, and finally reaches an approximate constant value around zero deep inside Ω_R. Furthermore, we have numerically confirmed the validity of $\sum_\alpha u_\alpha(\mathbf{r}) = 1$ given in Ref. 3.

To show that the current calculated from ac current density is conserved, we define the current across the cross section located at z:

$$I_\alpha(z) = \int dxdy\hat{\mathbf{z}} \cdot \mathbf{J}_\alpha(x,y,z), \tag{36}$$

where $\alpha = c,d,\mathrm{nl},t$. (The current and current density are plotted in units of $iq^2\Omega/h$.) Figure 4 depicts the different components of current while crossing different cross sections along z direction. We see that the total current I_t is a constant in Ω_C and equals to the emittance E_{LL}, i.e., $\nabla \cdot \mathbf{J}_t(\mathbf{r}) = 0$ in Ω_C region. As expected, the current I_t varies in the coupling regions Ω_L and Ω_R due to the presence of self-energy. Due to the current conservation condition $\sum_\alpha I_\alpha = 0$, the emittance

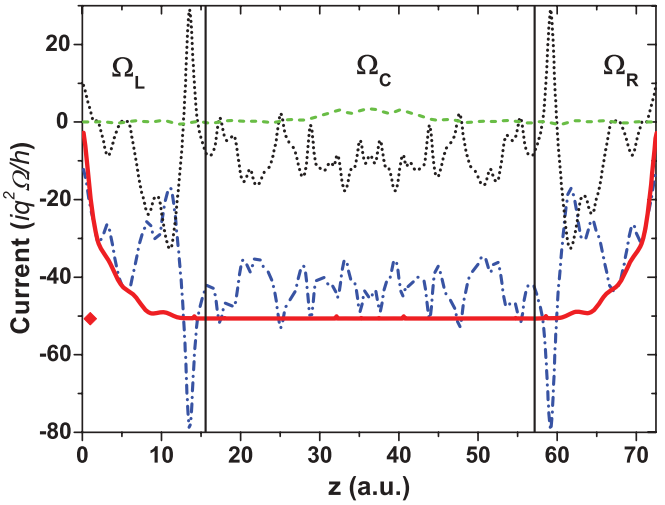

FIG. 4. (Color online) Conventional current I_c (blue dash dot line), displacement current I_d (green dash line), nonlocal current I_n (black dot line), and total current I_t (red solid line) transporting along z direction. Here, the red diamond symbol denotes the emittance E_{LL} calculated from the lead.

should satisfy the following equation:

$$\sum_\alpha E_{\alpha\beta} = 0. \tag{37}$$

Note that the emittance E_{LL} is negative, E_{RL} is positive, which indicates that the system shows inductive-like behavior.[3] This is understandable because the equilibrium transmission $T(E_f) = 0.87$, which means the system is transmissive.

Because the current density is a vector field, it can be projected on different slices along each direction for better visualization. Furthermore, we define x and z components of position-related total current density $\mathbf{J}_{t,p}(\mathbf{r})$ as the sum of several neighboring points in the same plane, i.e.,

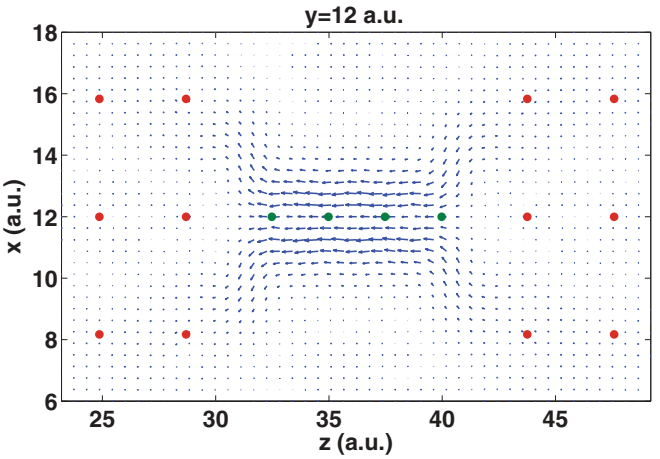

FIG. 5. (Color online) Distribution of the position-related current density $\mathbf{J}_p(\mathbf{r})$ in x-z plane in the central of y axis slices. The arrows indicate the magnitude and direction of current flow in each position. Red points represent Al atoms and green points represent C atoms projected into the x-z plane. $\mathbf{J}_p(\mathbf{r})$ is plotted in units of $iq^2\Omega/h$.

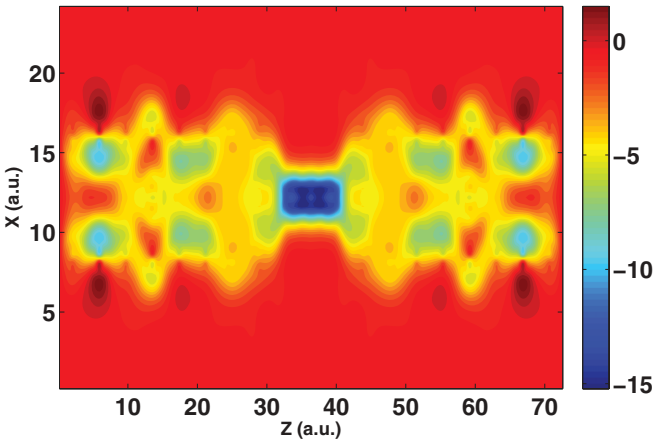

FIG. 6. (Color online) Numerical plot of z component of $\mathbf{J}_t$ in transverse x direction and transport z direction by the summation of values in y direction. $\mathbf{J}_t$ is plotted in units of $iq^2\Omega/h$.

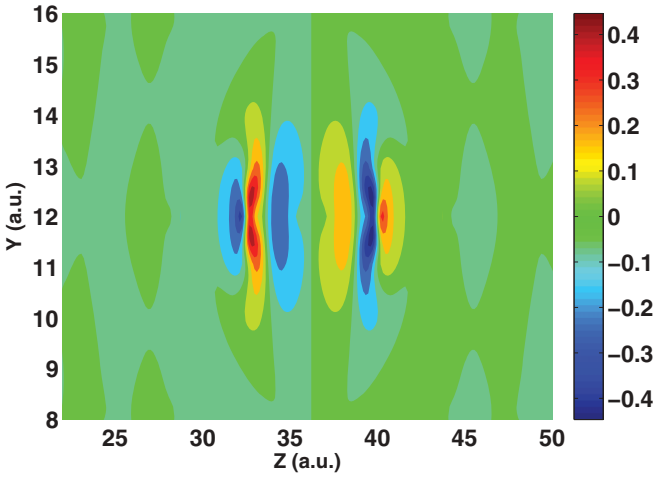

FIG. 7. (Color online) The nonequilibrium charge distribution $\rho_L(\mathbf{r})$ injected from the left lead on y-z plane. $\rho_L(\mathbf{r})$ on y-z plane is plotted in the atomic unit.

$\mathbf{J}^i_{t,p}(\mathbf{r}') = \sum_{\mathbf{r}}^{\mathbf{r}+2a_x} \sum_{\mathbf{r}}^{\mathbf{r}+4a_z} \mathbf{J}^i_t(\mathbf{r})$ and a_i is the unit length of real space grid, $i = x/z$. We cut a slice in y direction ($y = 12$ a.u.) to show the position-related total current density $\mathbf{J}_{t,p}(\mathbf{r})$. As you can see in Fig. 5 that ac current density flows in negative direction and mainly distributes around each atom. It can be clearly seen that the distribution of current density is due to the scattering from Al to the carbon atoms C in Fig. 5.

It is the z component of current density that dominates the transport properties of the molecular device. In Fig. 6, we depict the current density $\mathbf{J}_t$ of the whole system. The current density $\mathbf{J}_t$ surrounding four carbon atoms is highly negative compared with other regions, which confirms that the carbon atoms are conductive.

In addition, we studied the nonequilibrium charge distribution due to the ac bias. In Fig. 7, we have shown the charge density $\rho_L(\mathbf{r})$ injected from the left lead in yz plane by taking the average in the x direction. One can see that the nonequilibrium charge density is polarized in the whole system. Furthermore, the polarization is symmetric about the center of z axis. It is natural to divide the system into two regions $\Omega_{1,2}$ according to this symmetry axis. Correspondingly, the quantum electrochemical capacitance $C = \int_{\Omega_1} \rho_L(\mathbf{r}) d\mathbf{r}$ is equal to $C = 0.02$ aF.[38]

IV. SUMMARY

In summary, we have developed a formalism to calculate ac current density using NEGF formalism. We have shown that in order to conserve the ac current density, the displacement current density must be included explicitly in addition to the Coulomb interaction. This is very different from the ac current calculation. We have also shown that the ac current calculated by integrating the total ac current density derived from our theory across an arbitrary cross section inside the central scattering region is a constant and equals to the terminal current calculated directly from NEGF. We have implemented this formalism into a NEGF-DFT scheme. As an example, we have calculated the ac current density to the first order in frequency for a molecular device Al-C_4-Al from first principles. It is shown that the Al-C_4-Al system gives inductive-like behavior attributing to the transmissive nature of system in low-frequency limit. Finally, the nonequilibrium charge distribution is studied.

ACKNOWLEDGMENTS

We gratefully acknowledge the support from Research Grant Council (HKU 705611P) and University Grant Council (Contract No. AoE/P-04/08) of the Government of HKSAR.

APPENDIX: DERIVATIONS FOR DIFFERENTIAL CONVENTIONAL CURRENT DENSITY EXPRESSION

From Eqs. (4) and (26), we can obtain the expression of differential conventional current density. Firstly, we expand the nonequilibrium part of the lesser Green's function in terms of the first order in frequency and only keep the first order:

$$g_n^<(E_+,E)/[v_L(\Omega) - v_R(\Omega)] = iq\frac{f - f - \Omega f' - \Omega^2 \frac{f''}{2}}{\Omega}[(G^r - \Omega G^r G^r)(\Gamma_L G^a - \Gamma G^a u_L)]$$
$$= iq\Omega\left[f' G^r G^r(\Gamma_L G^a - \Gamma G^a u_L) - \frac{f''}{2} G^r(\Gamma_L G^a - \Gamma G^a u_L)\right] \quad \text{(A1)}$$

with $f' = \partial_E f$ and $f'' = \partial_E f'$. Then, the corresponding differential conventional current density up to the first order in frequency can be written as (not including the zeroth order)

$$\begin{aligned}\mathbf{J}_c(\mathbf{r},\Omega) &= \frac{iq^2\hbar\Omega}{2m}\int\frac{dE}{2\pi}(\nabla-\nabla')\Big[f' G^r G^r(\Gamma_L G^a - \Gamma G^a u_L) - \frac{f'}{2}(G^r G^r \Gamma_L G^a - G^r G^r \Gamma G^a u_L \\ &\quad + G^r \Gamma_L G^a G^a - G^r \Gamma G^a G^a u_L)\Big] \\ &= \frac{iq^2\hbar\Omega}{4m}\int\frac{dE}{2\pi}(-\partial_E f)[(\nabla-\nabla')(G^r\Gamma_L G^a G^a - G^r G^r \Gamma_L G^a + (G^r G^r \Gamma G^a - G^r \Gamma G^a G^a)_{\mathbf{rr}} u_L)]_{\mathbf{r}'=\mathbf{r}}, \qquad \text{(A2)}\end{aligned}$$

where we have used the integration by parts in the first equality.

*jianwang@hku.hk

[1] M. Bütiker, H. Thomas, and A. Prêtre, Phys. Lett. A **180**, 364 (1993).
[2] M. Büttiker, A. Prêtre, and H. Thomas, Phys. Rev. Lett. **70**, 4114 (1993).
[3] M. Büttiker, J. Phys.: Condens. Matter **5**, 9361 (1993).
[4] M. H. Pedersen, S. A. van Langen, and M. Büttiker, Phys. Rev. B **57**, 1838 (1998).
[5] N. S. Wingreen, A. P. Jauho, and Y. Meir, Phys. Rev. B **48**, 8487 (1993).
[6] A. P. Jauho, N. S. Wingreen, and Y. Meir, Phys. Rev. B **50**, 5528 (1994).
[7] C. Bruder and H. Schoeller, Phys. Rev. Lett. **72**, 1076 (1994).
[8] T. H. Oosterkamp, L. P. Kouwenhoven, A. E. A. Koolen, N. C. van der Vaart, and C. J. P. M. Harmans, Phys. Rev. Lett. **78**, 1536 (1997).
[9] T. H. Oosterkamp, T. Fujisawa, W. G. van der Wiel, K. Ishibashi, R. V. Hijman, S. Tarucha, and L. P. Kouwenhoven, Nature **395**, 873 (1998).
[10] J. Gabelli, G. Fève, J.-M. Berroir, B. Plaçis, A. Cavanna, B. Etienne, Y. Jin, and D. C. Glattli, Science **313**, 499 (2006).
[11] G. Fève, A. Mahé, J.-M. Berroir, T. Kontos, B. Plaçis, D. C. Glattli, A. Cavanna, B. Etienne, and Y. Jin, Science **316**, 1169 (2007).
[12] S. Hermelin, S. Takada, M. Yamamoto, S. Tarucha, A. D. Wieck, L. Saminadayar, C. Bäerle, and T. Meunier, Nature (London) **477**, 435 (2011).
[13] R. P. G. McNeil, M. Kataoka, C. J. B. Ford, C. H. W. Barnes, D. Anderson, G. A. C. Jones, I. Farrer, and D. A. Ritchie, Nature (London) **477**, 439 (2011).
[14] S. E. Nigg, R. Lopez, and M. Buttiker, Phys. Rev. Lett. **97**, 206804 (2006).
[15] J. Wang, B. G. Wang, and H. Guo, Phys. Rev. B **75**, 155336 (2007).
[16] C. Mora and K. Le Hur, Nat. Phys. **6**, 697 (2010).
[17] S. Li, Z. Yu, S.-F. Yen, W. C. Tang, and P. J. Burke, Nano Lett. **4**, 753 (2004).
[18] L. Gomez-Rojas, S. Bhattacharyya, E. Mendoza, D. C. Cox, J. M. Rosolen, and S. R. P. Silva, Nano Lett. **7**, 2672 (2007).
[19] J. Chaste, L. Lechner, P. Morfin, G. Feve, T. Kontos, J.-M. Berroir, D. C. Glattli, H. Happy, P. Hakonen, and B. Placais, Nano Lett. **8**, 525 (2008).
[20] Q. F. Sun, J. Wang, and T. H. Lin, Phys. Rev. B **61**, 12643 (2000).
[21] M. P. Anantram and S. Datta, Phys. Rev. B **51**, 7632 (1995).
[22] B. G. Wang, J. Wang, and H. Guo, Phys. Rev. Lett. **82**, 398 (1999).
[23] Y. D. Wei and J. Wang, Phys. Rev. B **79**, 195315 (2009).
[24] In the Coulomb blockade regime, the quantum transport problem has been treated by a number of groups. See Refs. 25–28 for details.
[25] R. Stadler, V. Geskin, and J. Cornil, Phys. Rev. B **78**, 113402 (2008).
[26] R. Stadler, V. Geskin, and J. Cornil, Phys. Rev. B **79**, 113408 (2009).
[27] S. Kurth, G. Stefanucci, E. Khosravi, C. Verdozzi, and E. K. U. Gross, Phys. Rev. Lett. **104**, 236801 (2010).
[28] C. D. Spataru, M. S. Hybertsen, S. G. Louie, and A. J. Millis, Phys. Rev. B **79**, 155110 (2009).
[29] J. L. Wu, B. G. Wang, J. Wang, and H. Guo, Phys. Rev. B **72**, 195324 (2005).
[30] B. Wang and J. Wang, Phys. Rev. B **77**, 245309 (2008).
[31] C. S. Li, L. H. Wan, Y. D. Wei, and J. Wang, Nanotechnology **19**, 155401 (2008).
[32] L. Zhang, B. Wang, and J. Wang, Phys. Rev. B **84**, 115412 (2011).
[33] J. Taylor, H. Guo, and J. Wang, Phys. Rev. B **63**, 245407 (2001); **63**, 121104 (2001).
[34] D. Waldron, P. Haney, B. Larade, A. MacDonald, and H. Guo, Phys. Rev. Lett. **96**, 166804 (2006).
[35] D. Waldron, V. Timoshevskii, Y. Hu, K. Xia, and H. Guo, Phys. Rev. Lett. **97**, 226802 (2006).
[36] N. Troullier and J. L. Martins, Phys. Rev. B **43**, 1993 (1991).
[37] M. Büttiker and T. Christen, in *Quantum Transport in Semiconductor Submicron Structures*, edited by B. Kramer (Kluwer Academic Publishers, Dordrecht, 1996), p. 263.
[38] J. Wang, H. Guo, J.-L. Mozos, C. C. Wan, G. Taraschi, and Q. R. Zheng, Phys. Rev. Lett. **80**, 4277 (1998).